Biodistribution properties of cleistanthin A and cleistanthin B using magnetic resonance imaging in a normal and tumoric animal model

Subramani Parasuraman, Ramasamy Raveendran, Mehdi Shafiee Ardestani[1], Ananthakrishnan Ramesh[2], Ali Jabbari-Arabzadeh[1], Mohammad Shafiee Alavidjeh[1], Mohammad Reza Aghasadeghi[1], Sundararajan Elangovan[2], Halanaik Dhanapathi[3]

Departments of Pharmacology, [2]Radiodiagnosis and [3]Nuclear Medicine, Jawaharlal Institute of Postgraduate Medical Education and Research, Pondicherry, India, [1]Nanobiotechnology and Hepatitis B/AIDs, Pasteur Institute of Iran, Tehran, Iran

Submitted: 23-08-2011 Revised: 05-10-2011 Published: 23-05-2012

ABSTRACT

Aim: To determine the biodistribution properties of cleistanthin A and cleistanthin B in rodents using magnetic resonance imaging (MRI). **Materials and Methods:** Cleistanthins A and B, constituents of *Cleistanthus collinus* Roxb., were labelled with gadolinium (Gd^{3+}) directly and injected into normal and tumoric nude mice. The tissue signal intensity was measured using MRI to perform a noninvasive kinetic assay. Wistar rats were used for determination of the grayscale intensity to observe the distribution patterns of of cleistanthins A and B. **Results:** Cleistanthin A is kinetically more attractive to the gastrointestinal tract than is cleistanthin B, which gets accumulated in muscular tissues of mice in greater concentrations compared with cleistanthin A. Cleistanthin B but not cleistanthin A showed tumoric affinity and exhibited a tumor kinetic attraction in tumoric mice. In rats, cleistanthin A showed greater grayscale intensities in the brain, liver, and skeletal muscles in immediate post contrast MRI images, whereas the gadolinium tagged cleistanthin B showed higher grayscale intensities in the cardiac muscle and skeletal muscles in delayed post contrast MRI images. **Conclusions:** Cleistanthin A is more pharmacokinetically attractive to the gastrointestinal tract than cleistanthin B.

Key words: Biodistribution, cleistanthin A, cleistanthin B, magnetic resonance imaging

Access this article online

Website: www.phcog.com

DOI: 10.4103/0973-1296.96559

Quick Response Code:

INTRODUCTION

Cleistanthin A and cleistanthin B are two of the many constituents of the leaves of *Cleistanthus collinus* Roxb. (Euphorbiaceae). This plant is commonly used as a suicidal and homicidal poison in Southeast Asian countries,[1] and cleistanthins A and B have been reported to be responsible for toxic effects in human beings.[2,3] Arylnaphthalide lignin glycosides are the major phytoconstituent of the genus *Cleistanthus*. They are also present in *Phyllanthus taxodiifolius*, *Haplophyllum buxbaumii*, and *Cleistanthus patulus*.[4] Although cleistanthins A and B have been reported to produce toxicity, the distribution patterns of the compounds and its significance have not been reported.

Address for correspondence:
Dr. S. Parasuraman, Department of Pharmacology, Jawaharlal Institute of Postgraduate Medical Education and Research, Pondicherry, India. E-mail: parasuphd@gmail.com

This study was designed to determine the distribution pattern, accumulation sites, tissue binding nature and possible absorption and excretion patterns of cleistanthins A and B in rodents after administering gadolinium (medical diagnostic contrast) tagged compounds and examining them under a magnetic resonance imaging (MRI) system.

MATERIALS AND METHODS

This collaborative study was conducted in the departments of Pharmacology, Radiology and Nuclear Medicine, Jawaharlal Institute of Postgraduate Medical Education and Research (JIPMER), Pondicherry, India, and at the Department of Nanobiotechnology and Hepatitis B/AIDS, Pasteur Institute of Iran, Tehran, Iran.

Plant material

Taxonomically identified *Cleistanthus collinus* Roxb.

(Euphorbiaceae) plant parts were collected in Pondicherry and in rural parts of Villupuram and Cuddalore districts of Tamil Nadu, India. They were identified and certified by the Botanical Survey of India (BSI), Coimbatore (reference number BSI/SC/5/23/08-09/Tech. 241). Leaves of *Cleistanthus collinus* were collected in the months of February–April every year. A voucher specimen of the plant is kept in the Department of Pharmacology, JIPMER, for further reference.

Isolation of cleistanthin A and cleistanthin B

Cleistanthin A and cleistanthin B were isolated from leaves of the *Cleistanthus collinus* plant. The acetone extract was obtained from defatted powered leaves. This extract was dissolved in benzene and passed through a neutral alumina column and eluted with a benzene and with benzene:ethyl acetate (4:1), benzene:ethyl acetate (1:1), and methanol:chloroform (9.5:0.5) mixtures to isolate fractions of fatty alcohol, collinusin, cleistanthin A, and cleistanthin B, respectively. The fractions of cleistanthin A and cleistanthin B were purified, and the functional groups and facial arrangements of the molecules were confirmed by spectroscopic analysis.[5-7]

Animals

Nude mice (16–20 g) and Wistar rats (150–180 g) of both sexes were used for the experiment. The nude mice were obtained from the Pasteur Institute of Iran and allowed to adapt to the laboratory conditions for a week. The Wistar rats were obtained from the central animal house of JIPMER, Pondicherry, and allowed to adapt to the laboratory conditions for a week. All the experimental animals were housed at a temperature of 21 ± 2 °C and 60–70% relative humidity in a 12:12 ± 1 h light–dark cycle. The animals were provided with an adequate standard rodent pellet diet and tap water *ad libitum*. The experimental protocol was approved by the local ethics committee of the Pasteur Institute of Iran, Tehran, Iran and Institute Animal Ethics Committee (IAEC) of JIPMER, Pondicherry, India. All the animal experiments were carried out in accordance with the guidelines of the Committee for the Purpose of Control and Supervision of Experiments on Animals (CPCSEA), India.

Tagging compounds

The direct labelling method was used for tagging cleistanthin A and cleistanthin B with gadolinium (Gd^{3+}). Two millimoles each of cleistanthin A and cleistanthin B were mixed with 2 mmol of meglumine in distilled deionized water. Meglumine (Pubchem CID: 8567) is an amino sugar derived from sorbitol and used to enhance visualization of tissues in medical imaging systems. The pH value of the mixture was adjusted to 7.5, and 5 mmol of vitamin C (antioxidant) was added with constant stirring for 10 min. Then, gadolinium chloride ($GdCl_3$, 1 mmol) was added drop by drop into the mixture. The preparation containing cleistanthin A/ cleistanthin B in meglumine, vitamin C, and $GdCl_3$ was incubated at room temperature with constant stirring for 2 h. The binding efficacy of cleistanthin A and cleistanthin B with $GdCl_3$ was assessed using thin layer chromatography (TLC) with remade silica gel as the stationary phase and ethanol:sulfuric acid (9.5:0.5) as the mobile phase.[8,9]

Confirmation of complex formation

Size-exclusive HPLC (SE-HPLC) was employed for analysis of the complex formed by cleistanthins A and B with gadolinium. The electrochemical detection (ECD) system consisted of a Shimadzu SCL 10-Avp system controller, LC-10AS pump, SIL-10A cooled autoinjector, CT0-10A oven, LECD-6A electrochemical detector, and Gastorr online degasser (ISS, England). Class VP-5 software (Shimadzu) was used with the system. All samples were injected into a reverse phase Luna 5 µm C_{18} 250 mm × 4.6 mm column (Phenomenex), which was protected by Krudkatcher disposable pre-column filters (Phenomenex) and Security Guard cartridges (Phenomenex).

A mixture of 0.1 M disodium hydrogen orthophosphate and 50 µM EDTA (pH 5.6, 1 M OPA) and HPLC grade methanol (35:65) was used as the mobile phase. This mobile phase was filtered through Millipore 0.45 µm HV Durapore membrane filters (AGB, Dublin) and vacuum degassed prior to use. Compounds were eluted isocratically over a 20 min runtime at a flow rate of 0.65 ml/min after a 20 µl injection. The column was maintained at a temperature of 30 °C, and samples/standards were maintained at 4 °C in the autoinjector prior to analysis unless otherwise stated. The glassy carbon working electrode, combined with an Ag/AgCl reference electrode (Shimadzu), was operated at +0.8 V unless otherwise specified, and the range of the detector was set to 1.

Quantitative data analysis

T1- and T2-weighted SE images at 1.5 *T* (TR/TE = 250 ms/16 ms and TR/TE = 4000 ms/64 ms) were analysed qualitatively. The signal intensities of vials with contrast medium in solution and contrast medium in cells with corresponding iron concentrations were visually compared.

The magnetic resonance (MR) images were transferred as DICOM (Digital Imaging and Communications in Medicine) images to DICOM Works software (Phillipe Puech and Loic Boussel. v 1.3.5). For each concentration, triplicate sampling and the maximum region of interest were considered.

All imaging protocols were done on a 1.5 T GE MRI (Sigma)

system. The relaxation rates of gadolinium-loaded-complex contrast agents were measured for different concentrations of the gadolinium-loaded-complex samples, using different spin echo (SE) and gradient echo (GE) protocols. For T2 measurement, two multi-echo SE protocols were used with echo time (TE) values of 12, 24, 36, and 48 ms and 46, 92, 138 and 184 ms, respectively (repetition time [TR] =1000 ms) (Equation 1).

$$\text{Signal}_{SE} = S_0 e^{-R_2 TE}) \quad (1)$$

TR-variable SE imaging (with the same TE values) was used for T1 measurement. For T2 measurement, multi-echo SE protocols were used with TR values of 60, 140, 240, 340, 440, 600, 800, 1000, 1500, 2000, 3000, and 5000 ms (TE = 11 ms). The signal intensity equation used for T1 measurement was as follows:

$$\text{Signal}_{SE} = S_0(1 - e^{-TR/T_1}) \quad (2)$$

T1 and T2 maps were calculated assuming a monoexponential signal decay. T1 maps were calculated from four SE images with a fixed TE of 11 ms at 1.5 T and TR values of 60, 140, 240, 340, 440, 600, 800, 1000, 1500, 2000, 3000, and 5000 ms using a nonlinear function least-square curve fitting on a pixel-by-pixel basis. The signal intensity of each pixel as a function of time was expressed as follows: SIpixel $xy(t)$ = So(pixel xy) [1 − exp (−t/T1pixel xy)].[10]

T2 maps were calculated accordingly from four SE images with a fixed TR and TE values of 12, 24, 36, and 48 ms. The signal intensity for each pixel as a function of time was expressed as follows: SIpixel $xy(t)$ = So (pixel xy) exp (t/T2pixel xy). Care was taken to analyse only data points with signal intensities significantly above the noise level. The T1 and T2 relaxation times (s) of the samples in the Eppendorf tubes were obtained from ROI measurements of the test samples on these T1 and T2 maps, and the results were converted to R1 and R2 relaxation rates (s^{-1}).

Cancer animal model

Nude mice were xenografted in the right foreleg muscle with 4 × 10^6 human non-small-cell lung cancer [NSCLC] cells. Two weeks later, the tumors attained a size of about 4 mm (diameter).

In vivo imaging of cleistanthin A and cleistanthin B

Nude mice (16–20 g) of either sex were used for the study. Each animal was anaesthetized with ketamine (50 mg/kg) and xylazine (5 mg/kg).[11,12] The tail vein was cannulated, and 20 mg/kg of tagged cleistanthin A/cleistanthin B was injected. The animal was then placed in a clinical MRI apparatus (1.5 T, GE Sigma). T1-weighted MRI procedures were performed prior to and 20 min after injection. The imaging procedures were also performed on tumoric nude mice.

Determination of grayscale intensity

The grayscale intensity is a measure of the intensity of light at each pixel in a single band of the electromagnetic spectrum. A fasted male rat (8–10 h) was anesthetized using ketamine (80 mg/kg, i.p.) and xylazine (16 mg/kg, i.p.). The animal was placed on a surgical platform, and the skin on the right thigh was exposed and disinfected. A small incision was made in the right thigh, the femoral vein was identified, and cannulated with a 26G × 1/2" needle, and 20 mg/kg of tagged cleistanthin A or cleistanthin B was injected.[11,12] The animal was placed in a clinical MRI apparatus (1.5 T, Siemens, Germany). A delayed post-contrast image was taken 30 min after i.v. injection of plain gadolinium as Gadobenate Dimeglumine (MultiHance®). The pre-contrast, immediate, and delayed post-contrast images were taken for all the animals. The grayscale intensities were calculated for all the animals, and the difference in intensity was determined between the pre-contrast and immediate post-contrast images and between the pre-contrast and delayed post-contrast images. The mean ± SD signal intensity values were calculated for a region of interest with an area of 1.0–1.2 sq. cm, comprising around 35–40 pixels.

RESULTS

The binding efficacies of cleistanthin A and cleistanthin B with gadolinium were 82% and 78%, respectively [Figure 1]. The T1 relaxivity values of cleistanthins A and B at 37°C were 62.5 and 60.3 mM s^{-1}, respectively. The T2 relaxivity values of cleistanthin A and B at 37°C were 24.4 and 22.1 mM s^{-1}, respectively. The ratio of R2 to R1 for cleistanthins A and B were 2.56 and 2.88, respectively. It can be seen that cleistanthins A and B caused a decrease in both the relaxation times T1 and T2 compared with Magnevist® and water [Figure 2]. The T1 and T2 relativity values (calculated from Equations (1) and (2)) are shown in Table 1. The *in vitro* studies showed the relaxivity values of cleistanthins A and B to be 62.5 and 60.3 mM^{-1} s^{-1} relaxivity for Cleistanthins A and B, respectively.

A schematic illustration of the performance of *in vitro* T1/T2 measurements using an MRI apparatus is shown in Figure 3. For each concentration, triplicate sampling and the maximum region of interest were considered. Five concentrations of tagged cleistanthin A and cleistanthin B (0.33, 0.17, 0.08, 0.04, and 0.02 mmol/mL) were obtained by dilution with 0.9% sodium chloride. The *in vivo* drug distribution patterns in normal and cancer nude mice were obtained 20 min after injection (i.v.) of tagged cleistanthin A or cleistanthin B and are presented in Figures 4–6. The *in vivo* drug distribution study with 1.5 T MRI showed that (a)

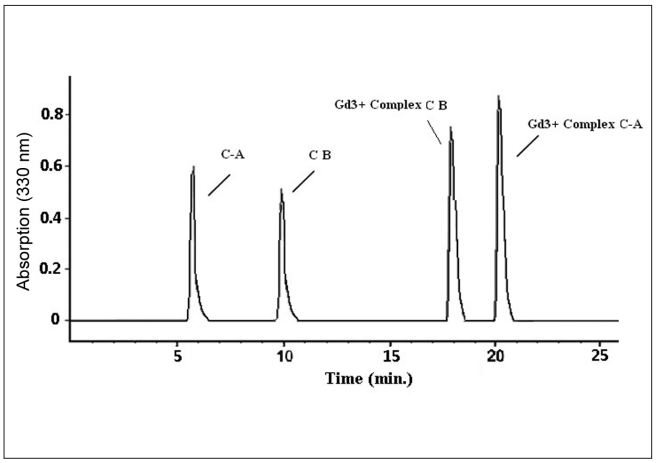

Figure 1: SE-HPLC chromatogram of cleistanthin A and cleistanthin B and their Gd^{3+} loaded analogues. The peak at 6 min is related to cleistanthin A, the one at 10 min is related to cleistanthin B, the one at 18 min is related to the cleistanthin B Gd^{3+}-loaded complex, and the last is attributed to the cleistanthin A Gd^{3+}-loaded complex analogue eluted at 20 min postinjection. The data were superimposed

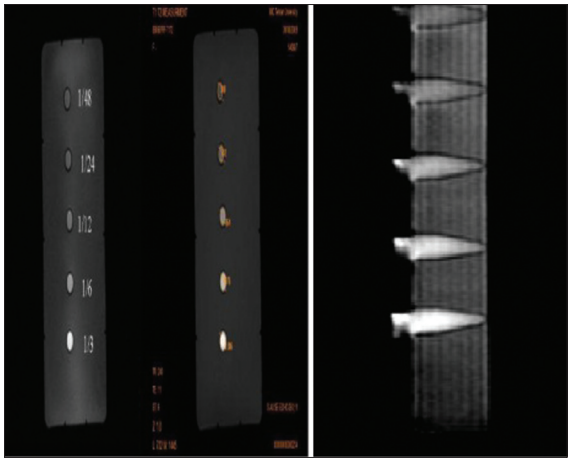

Figure 3: Schematic illustration of performance of *in vitro* T1/T2 measurements using a magnetic resonance imaging apparatus

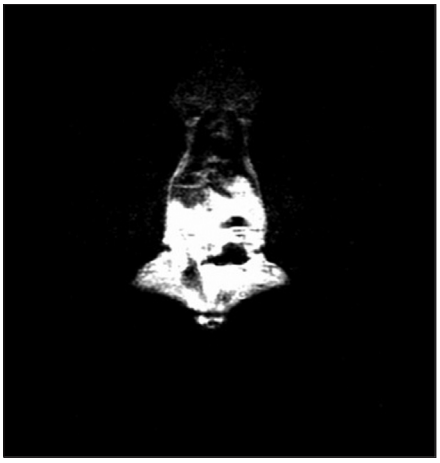

Figure 5: MRI (1.5 T) of normal nude mice 20 min after i.v. injection of cleistanthin B labeled with Gd^{3+}(20 μg/kg)

Figure 2: Relaxation data for Magnevist® control

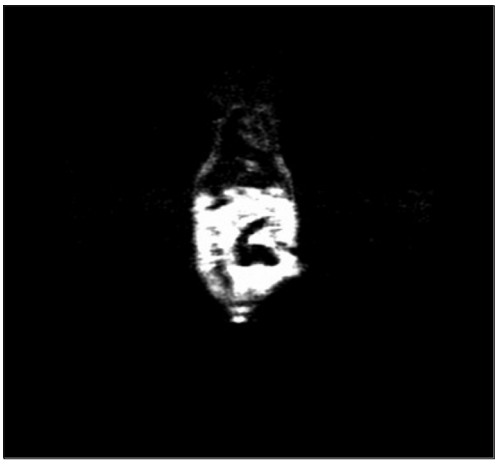

Figure 4: MRI of normal mice 20 min after injection of cleistanthin A labeled with Gd^{3+} (20 μg/kg)

Table 1: T1 and T2 values (in milliseconds) derived from Equations (1) and (2)

	1/3C	1/6C	1/12C	1/24C	1/48C	Water
Cleistanthin A T1	124	221	328	503	618	1363
Cleistanthin A T2	109	170	270	423	478	858
Cleistanthin B T1	106	202	298	482	588	1364
Cleistanthin B T2	100	164	255	402	422	859

cleistanthin A was more pharmacokinetically attractive to the gastrointestinal tract compared with cleistanthin B and that (b) cleistanthin B is being increasingly accumulated in muscular tissues rather than cleistanthin A.

The difference in grayscale intensity is presented in Tables 2 and 3 and in Figures 7 and 8. While the gadolinium tagged cleistanthin A showed greater grayscale intensities in the brain, liver, and skeletal muscles under immediate MRI, the gadolinium tagged cleistanthin B showed greater grayscale

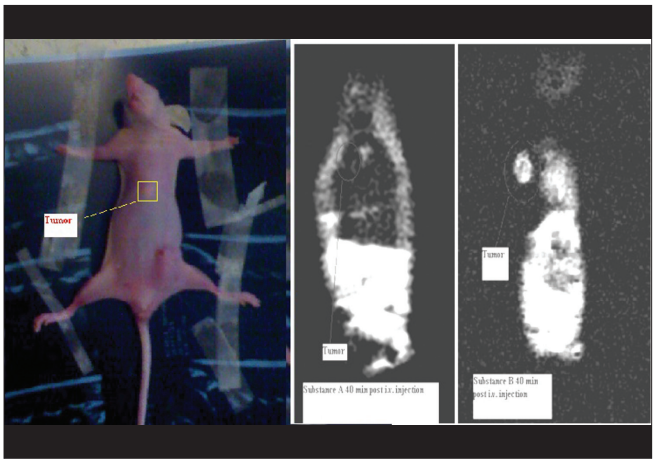

Figure 6: MRI (1.5 T) of tumoric nude mice 20 min after i.v. injection of cleistanthin A and cleistanthin B labeled with Gd^{3+} (20 µg/kg)

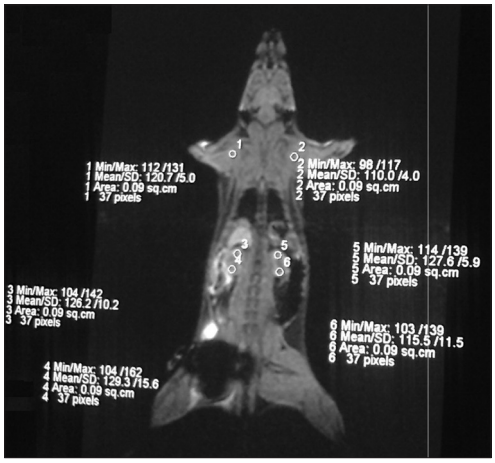

Figure 7: MRI of normal rat immediately after i.v. injection of cleistanthin A labeled with Gd^{3+} (20 µg/kg)

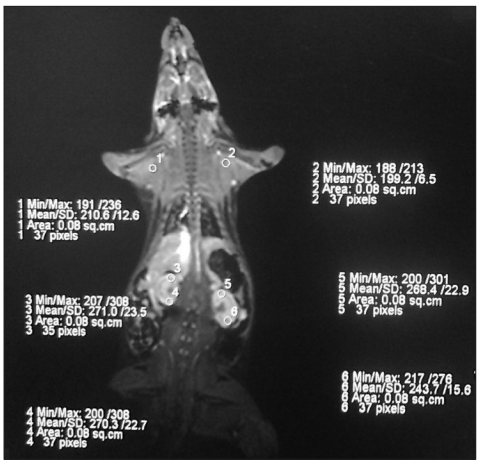

Figure 8: MRI of normal rat 30 min after i.v. injection of cleistanthin B labeled with Gd^{3+}(20 µg/kg)

intensities in the cardiac muscle and skeletal muscles under delayed MRI.

Table 2: Immediate post-contrast graysale intensities of cleistanthins A and B labeled with Gd^{3+}

	Control (injected with only Gd^{3+})	Cleistanthin A labeled with Gd^{3+}	Cleistanthin B labeled with Gd^{3+}
Brain	39.15 ± 16.74	67.80 ± 7.94	30.38 ± 11.58
Skeletal muscle	102.85 ± 31.90	91.87 ± 8.56	49.45 ± 18.43
Cardiac muscle	184.70 ± 69.09	52.47 ± 16.71	94.83 ± 58.57
Liver	179.15 ± 8.83	227.95 ± 23.53	124.50 ± 20.42
Kidney	279.30 ± 33.10	253.58 ± 18.24	114.18 ± 20.27
Bowel	164.83 ± 15.74	172.85 ± 7.96	54.60 ± 35.93

All the values are expressed as the mean ± SEM. The number of animals used in the experiment was three and the number of observations was six. The difference was calculated by comparing the plain and contrast values. Immediate post-contrast images were taken immediately after i.v. injection of plain gadolinium/gadolinium tagged with cleistanthin A or cleistanthin B

Table 3: Delayed post-contrast graysale intensities of cleistanthins A and B labeled with Gd^{3+}

	Control	Cleistanthin A labeled with Gd^{3+}	Cleistanthin B labeled with Gd^{3+}
Brain	86.23 ± 12.09	72.53 ± 18.97	34.63 ± 19.39
Skeletal muscle	103.40 ± 9.97	83.60 ± 11.72	140.45 ± 7.63
Cardiac muscle	147.03 ± 49.46	54.98 ± 26.17	248.55 ± 35.55
Liver	202.45 ± 33.18	148.22 ± 26.36	185.48 ± 27.58
Kidney	197.95 ± 3.01	184.30 ± 6.58	206.30 ± 24.60
Bowel	126.98 ± 37.19	124.47 ± 4.50	142.30 ± 4.92

All the values are expressed as the mean ± SEM. The number of animals used for the experiment was 3, and the number of observations was 6. The difference was calculated by comparing the Plain and contrast values. Delayed post-contrast images were taken 30 min after i.v. injection of plain gadolinium/gadolinium tagged with cleistanthin A or cleistanthin B

DISCUSSION

This study suggests that both cleistanthin A and cleistanthin B get accumulated in the gastrointestinal tract. Compared with cleistanthin B, cleistanthin A was found in greater quantities in the gastrointestinal tract, and this may be due to differences in the physicochemical properties of the compounds. The same could be the reason for cleistanthin B getting accumulated in muscular tissues in larger quantities compared with cleistanthin A.[13] The accumulation of cleistanthin A and cleistanthin B indicates that these compounds can be absorbed through oral administration. Gastric erosions were reported in patients with *Cleistanthus collinus* poisoning, and this could be due to accumulation of cleistanthin A and cleistanthin B in the stomach wall. Cleistanthins A and B have been reported to have anticancer effects, and the cytotoxic effects of the

accumulated cleistanthins A and B could be the reason for the erosions. Computer-aided tools also predicted that cleistanthins A and B could be absorbed through the gastrointestinal tract by passive diffusion, yielding an oral bioavailability of 30–70% and 30%, respectively.[14]

MRI helps demonstrate the behaviours of gastrointestinal, topical, colloidal, and target drug delivery systems.[15] The grayscale intensity calculation suggests that cleistanthin A is distributed immediately after i.v. administration and gets accumulated in the brain, liver, and skeletal muscles. However, cleistanthin B is distributed slowly after i.v. administration and gets accumulated in the cardiac muscle and skeletal muscles. The MRI of rats and mice indicates that both the compounds are excreted through the kidneys. The results suggest that cleistanthin B has a slow systemic distribution ratio, which may be attributed to differences in the physicochemical properties of the compounds.

CONCLUSION

This study leads to the conclusion that both cleistanthin A and cleistanthin B are accumulated in the gastrointestinal tract and distributed to the entire body. While cleistanthin A is accumulated in the brain, liver, and skeletal muscles, cleistanthin B is accumulated in the cardiac muscle and skeletal muscles. Cleistanthin A is pharmacokinetically more attractive to the gastrointestinal tract than is cleistanthin B, which is accumulated in muscular tissues in large quantities.

REFERENCES

1. Eswarappa S, Chakraborty, AR, Palatty BU, Vasnaik M. *Cleistanthus collinus* poisoning: case reports and review of the literature. Clin Toxicol 2000;41:369-72.
2. Annapoorani KS, Damodaran C, Chabdrasekharan P. High pressure liquid chromatographic separation of aryl-naphthalide lignan lactones. J Liq Chromatogr 1985;8:1173-94.
3. Annapoorani KS, Periakali P, Ilangovan S, Damodaran C, Sekharan PC. Spectrofluorometric determination of the toxic constituents of *Cleistanthus collinus*. J Anal Toxicol 1984;8: 182-6.
4. Pinho PM, Kijjoa A. Chemical constituents of the plants of the genus *Cleistanthus* and their biological activity. Phytochem Rev 2007;6:175-82.
5. Govindachari TR, Sathe SS, Viswanathan N, Pai BR, Srinivasan M. Chemical constituents of *Cleistanthus collinus* (Roxb.). Tetrahedron 1969;25:2815-21.
6. Parasuraman S, Raveendran R, Vijayakumar B, Velmurugan D, Balamurugan S. Molecular docking and *ex vivo* pharmacological evaluation of constituents of the leaves of *Cleistanthus collinus* (Roxb.) (Euphorbiaceae). Indian J Pharmacol 2012;44:197-203.
7. Parasuraman S, Raveendran R. Effect of cleistanthin A and B on adrenergic and cholinergic receptors. Pharmacogn Mag 2011;7:243-7.
8. Parmelee DJ, Walovitch RC, Ouellet HS, Lauffer RB. Preclinical evaluation of the pharmacokinetics, biodistribution, and elimination of MS-325, a blood pool agent for magnetic resonance imaging. Invest Radiol 1997;32:741-7.
9. Amanlou M, Siadat SD, Ebrahimi SE, Alavi A, Aghasadeghi MR, Ardestani MS, *et al*. Gd(3^{+})-DTPA-DG: novel nanosized dual anticancer and molecular imaging agent. Int J Nanomedicine 2011;6:747-63.
10. Simon GH, Bauer J, Saborovski O, Fu Y, Corot C, Wendland MF, *et al*. T1 and T2 relaxivity of intracellular and extracellular USPIO at 1.5T and 3T clinical MR scanning. Eur Radiol 2006;16:738-45.
11. Vogel HG. Drug Discovery and Evaluation: Pharmacological Assay. 3rd ed. Berlin: Springer; 2007.
12. Parasuraman S, Raveendran R, Kesavan R. Blood sample collection in small laboratory animals. J Pharmacol Pharmacother 2010;1:87-93.
13. Soine W. Hypnotics. In: Foye WO, Lemke TL, Williams DA, editors. Foye's Principles of Medicinal Chemistry. 6th ed. Baltimore: Lippincott Williams and Wilkins; 2002. p. 379-81.
14. Parasuraman S, Raveendran R. Computer-aided prediction of biological activity spectra, pharmacological and toxicological property of cleistanthin A and B. Int J Res Pharma Sci 2010;1:333-7.
15. Richardson CJ, Bowtell RW, Mäder K, Melia CD. Pharmaceutical applications of magnetic resonance imaging (MRI). Adv Drug Deliv Rev 2005;57:1191-209.

Cite this article as: Parasuraman S, Raveendran R, Ardestani MS, Ananthakrishnan R, Jabbari-Arabzadeh A, Alavidjeh MS, *et al*. Biodistribution properties of cleistanthin A and cleistanthin B using magnetic resonance imaging in a normal and tumoric animal model. Phcog Mag 2012;8:129-34.

Source of Support: Nil, **Conflict of Interest:** None declared.